

Bulk and interfacial thermodynamics of mixtures: From aqueous systems to ultracryogenic fluids

This document is an extended abstract of the PhD thesis entitled “Bulk and interfacial thermodynamics of mixtures: From aqueous systems to ultracryogenic fluids.” The PhD work was carried out by Ailo Aasen at the Department of Energy and Process Technology at the Norwegian University of Science and Technology from 1 January 2017 to 31 December 2019. Prof. Øivind Wilhelmsen served as the main supervisor and Dr. Morten Hammer served as the co-supervisor of the thesis work. The thesis defence took place on 27 March 2020, with Prof. Carlos Vega, Dr. Thijs van Westen, and Prof. Maria Fernandino as opponents.

SUMMARY AND PROBLEMS ADDRESSED

Understanding and modeling the thermodynamics of bulk phases is of immense practical importance and receives a lot of attention by the scientific community. When two such phases coexist in stable or metastable equilibrium, an interfacial region forms, with an associated surface tension. Knowledge of the surface tension is crucial to model processes such as nucleation. This work is a theoretical study of both the thermodynamics of bulk phases as given by equations of state, as well as planar and curved surfaces separating two phases in stable or metastable equilibrium. Molecular simulations and experiments are also employed where relevant.

The first part of the thesis reviews capabilities and challenges with established equations of state (EoS). There are several criteria for the suitability of an EoS: accuracy in correlating measurements, thermodynamic consistency, computational speed, computational robustness, and predictive capability. Special attention is given to the most accurate EoS available, namely multiparameter EoS. Such EoS can exhibit artificial Maxwell loops in the two-phase region, which makes them numerically challenging to work with, and which prohibits their use in important applications such as the modeling of interfacial phenomena by density gradient theory. The most widely used class of EoS is cubic equations of state, owing to their low computational cost and good ability to correlate $PVTxy$ properties, although the description of liquid phase properties and caloric properties can be less satisfactory. Equations of state based on perturbation theory, such as those based on statistical associating fluid theory (SAFT), are preferred when predictive ability is important, or when few experimental data are available. An added benefit of approaches based on perturbation theory is that one obtains an accompanying molecular model and force field, which allows for studying the system using molecular simulation. Predictions of critical points with such theories are, however, often inaccurate. A range of different EoS are tested thoroughly on the carbon dioxide/water mixture, by fitting them to the same, thoroughly validated $PVTxy$ data. Comparing the models on the same basis facilitates a general discussion about their strengths and weaknesses.

We next turn to the development of an equation of state for ultracryogenic fluid mixtures, namely those consisting

of helium, neon, hydrogen and deuterium. Since these components have low masses and can exist in the liquid state below 50 K, they exhibit significant quantum effects and are also referred to as quantum fluids. There is a paucity of experimental measurements of thermodynamic properties of ultracryogenic mixtures, and none of the established models can accurately describe their properties. We develop an equation of state based on a third-order Barker–Henderson perturbation theory of the Helmholtz energy with quantum-corrected Mie pair potentials, called SAFT-VRQ Mie. The quantum corrections are modeled using the Feynman–Hibbs expansion, resulting in a molecular model in terms of mass- and temperature-dependent semiclassical force fields. SAFT-VRQ Mie and molecular simulations are used to obtain optimal parameters for the intermolecular potentials of neon, helium, deuterium, ortho-, para-, and normal- hydrogen, as well as binary interaction parameters for each pair of these components. Overall, we find the semiclassical force fields to be rather accurate, and in particular they yield a significantly more accurate representation than classical force fields.

The SAFT-VRQ Mie EoS is able to describe the thermodynamics of the semiclassical force fields also for mixtures, except in the critical region. By revisiting the fundamentals of perturbation theory for binary Lennard-Jones mixtures, we demonstrate that this breakdown does not stem from the use of quantum corrections, but rather from the representation of the second- and third-order perturbation term. We also evaluate different choices of hard-sphere reference mixtures, in particular pointing out that common approaches based on additive hard spheres are missing a contribution to the free energy.

The thesis next treats metastable phases, interfaces, and nucleation. The surface tension of a curved surface differs from its planar value, as described by the Tolman length (first-order correction) and the rigidity constants (second-order corrections) through the Helfrich expansion. We explain the general theory for this dependence for multi-component fluids, and calculate the Tolman length and rigidity constants for an ideal mixture (hexane–heptane) by use of density gradient theory. We show that the Tolman length of multicomponent fluids is independent of the choice of dividing surface, and present simple formulae that capture the change in the rigidity constants for different choices of dividing surface. For mixtures, the Tolman length, the rigidity constants, and the accuracy of the Helfrich expansion depend on the choice of path

in thermodynamic state space along which droplets and bubbles are considered. We thoroughly explore this path dependence and identify a path that makes the expansion particularly accurate.

These curvature corrections are next incorporated in multicomponent nucleation theory. The theory is applied to condensation in binary mixtures of alkanols and water, in which case classical nucleation theory (CNT) predicts an unphysical negative number of water molecules in the critical embryo. We show how to remove this inconsistency by accounting for the curvature dependence of the surface tension of the mixture. To that end, we determine the Tolman lengths and the rigidity constants for the ethanol–water and 1-propanol–water mixtures at 260 K by combining density gradient theory with an accurate equation of state. By properly incorporating the curvature corrections into CNT for multicomponent systems, we demonstrate that the resulting theory is free of physical inconsistencies. In particular, for the ethanol–water and 1-propanol–water mixtures, the average error in the predicted nucleation rates is reduced from 11–15 orders of magnitude to below 1.5.

Finally, the thesis discusses the heterogeneous crystallization of ice in supercooled binary liquids of alkanol and water. We develop a simple, semi-empirical model for the limit of supercooling before ice formation occurs. The model incorporates a parameter that is fitted to experiments for pure water, but is predictive for mixtures. The predicted limits of supercooling for alkanol–water mixtures are in reasonable agreement with experiments, but some systematic deviations are observed. The growth rate of ice crystals in pure water and alcohol solutions is also studied, and found to slow down by two orders of magnitude for mixtures containing only 2% ethanol compared to the growth rate in pure water.

The two key innovations of the thesis are (I) the development of a new modeling framework for mixtures of ultracryogenic fluids, and (II) the theory and numerical framework for handling curvature expansions of droplets and bubbles in mixtures. These will now be discussed in more detail.

I. KEY INNOVATION: FORCE FIELDS AND EQUATION OF STATE FOR ULTRACRYOGENIC FLUIDS

A. Background and state of the art

For most substances of practical interest, the thermodynamic properties of the fluid phase can be deduced from a classical statistical mechanical point of view, either through the development of analytical expressions (e.g. perturbation approaches) or through direct molecular simulations of a representative intermolecular potential. Under certain conditions, however, the classical approxi-

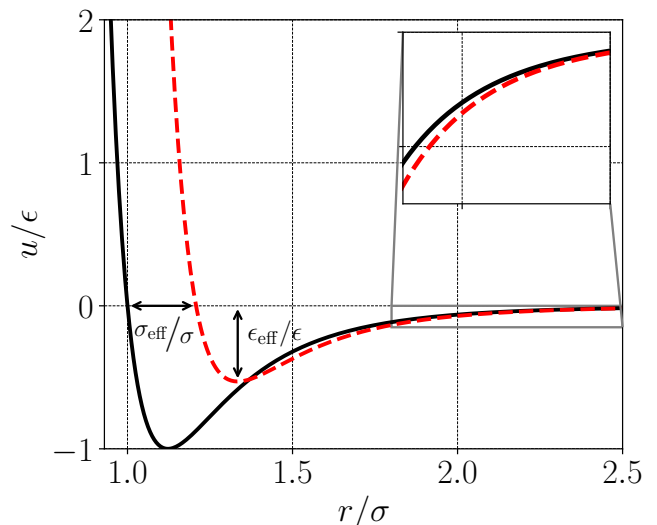


FIG. 1. Pair interaction potential for the Lennard-Jones (LJ) potential (black, solid line) and the LJ potential with second order Feynman–Hibbs (FH) quantum corrections (red, dashed). The temperature is given by $k_B T/\epsilon = 1$, and the particle mass is that of helium. The FH correction increases the effective diameter σ_{eff} , and decreases the well depth ϵ_{eff} , compared to the classical LJ parameters, σ and ϵ . The inset shows that the effective range of the potential increases slightly.

mations invoked break down and quantum effects start to become important. A typical gauge of the importance of quantum effects is the relative ratio of the de Broglie thermal wavelength, $\lambda_B = h/\sqrt{2\pi m k_B T}$, to the typical length scale across which particles interact. Here h and k_B are Planck’s and Boltzmann’s constants, m is the particle mass, and T is the temperature. It follows that non-classical effects should be strongest when particles have low mass, when temperatures are low, and when densities are high.

While in principle one could obtain the relevant average macroscopic properties through the solution of the Schrödinger equation, this is currently computationally infeasible for systems consisting of a large number of particles. Approximate treatments are therefore needed. Much effort was dedicated to this in the 1950s and 60s and significant progress was made. The Wigner–Kirkwood theory^{1,2} was the first to describe quantum corrections to classical interaction potentials, and this theory was elegantly re-derived and expanded upon by Feynman and Hibbs³ using the path-integral formulation of quantum mechanics. Its key idea is that classical statistical mechanics can still be used to describe particles experiencing quantum effects, given that they are taken to interact through effective, temperature-dependent potentials. The quantum-corrected potential takes the form as a series expansion in the thermal wavelength, and to first-order

the effective potential is given by

$$u_{\text{FH1}}(\mathbf{r}) = u_{\text{C}}(\mathbf{r}) + \frac{\lambda_{\text{B}}^2}{24\pi} \nabla^2 u_{\text{C}}(\mathbf{r}). \quad (1)$$

Here u_{C} is the classical potential, valid at high temperatures. Importantly, quantum corrections thus do not introduce any new fitting parameters into the potential. Qualitatively, the quantum corrections influence the pair potential in three ways, as illustrated in Fig. 1: the effective particle diameter increases, the effective potential well-depth decreases, and the range of the potential increases.

The start of the century brought renewed interest in the topic through the recognition that molecular simulations employing these *semiclassical* potentials could be used to study fluids such as helium, hydrogen and neon at low temperatures by use of classical molecular dynamics or Monte Carlo simulations. This simulation approach has since been used to study phenomena such as adsorption of hydrogen in porous materials^{4,5}, quantum clusters^{6,7}, helium at low temperatures⁸ and quantum fluids under confinement⁹. Two obstacles to this development, which the thesis aimed to overcome, were a lack of force fields whose range of validity included the VLE regime of the fluids, and the lack of force fields for mixtures.

The most accurate equations of state for pure helium, neon, hydrogen and deuterium are multiparameter EoS¹⁰. These EoS are, however, hampered by obstacles¹¹ that limit their range of application. For mixtures these obstacles are amplified, due to the absence of binary mixing models needed to extend multiparameter EoS to ultracryogenic fluid mixtures, as well as the sufficient experimental data to fit them. In fact, at the time of writing the thesis no accurate EoS existed for mixtures of ultracryogenic fluids. Wilhelmson et al.¹² tested several EoS for modeling the phase equilibria of helium–neon mixtures, such as cubic EoS with advanced mixing rules^{13–15}, sophisticated corresponding-states EoS such as SPUNG¹⁶, and PC-SAFT¹⁷. None of these EoS yielded good agreement with measurements.

B. Method and results

We developed an equation of state for generic Mie-fluids with first (Mie-FH1) and second-order Feynman–Hibbs corrections (Mie-FH2). The EoS is based on perturbation theory with a third-order Barker–Henderson expansion of the Helmholtz energy. One aspect of perturbation theory worked to our advantage when tackling the ultracryogenic fluids: it is expected to converge faster for potentials with a steep repulsion and a weak and long attractive tail¹⁸. In fact, Feynman–Hibbs corrections have precisely the effect of making potentials have steeper repulsion and longer shallower tails, making perturbation theory particularly powerful for such potentials.

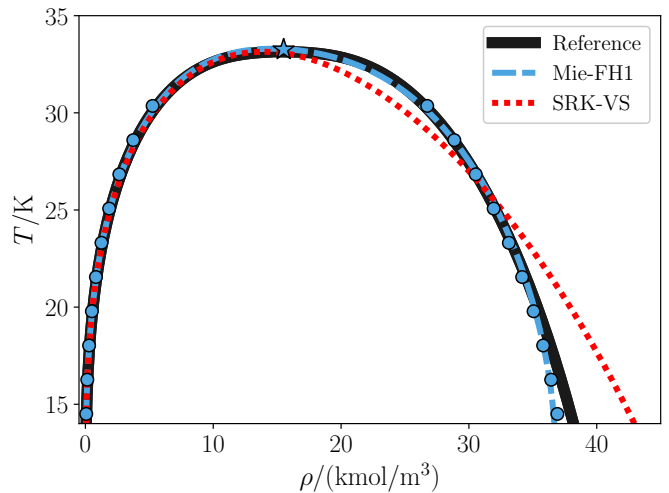


FIG. 2. Phase diagram for pure hydrogen from simulations, EoS calculations, and experiments. Dots are simulation results with the optimized semiclassical force field, where the star is a scaling-law estimate of the critical point. The dashed blue curve is the SAFT-VRQ Mie equation of state developed in the thesis, and the black curve is a correlation of the experimental phase diagram. The red dotted curve illustrates the performance for a cubic EoS: SRK with volume shift.

Having developed the theory for generic Mie-FH1 and Mie-FH2 potentials, we next exploited the one-to-one correspondence between the EoS and the interaction potentials to find the optimal force-field parameters to represent the thermodynamic properties of pure neon, helium, normal-hydrogen, ortho-hydrogen, para-hydrogen and deuterium. The optimization procedure minimized deviations for a range of properties: saturation densities and pressures, saturated and supercritical heat capacities, supercritical speeds of sound, and the critical point. Excellent agreement was achieved, as illustrated for pure hydrogen in Fig. 2.

The cross interaction potential between different components had to be optimized based on a sparser amount of data, and were fitted to cross second virial coefficients and phase composition measurements of binary mixtures of the ultracryogenic fluids helium, neon, hydrogen and deuterium. Good agreement was achieved for the force field simulations for all mixtures, as exemplified in Fig. 3. Some deviations were observed for the perturbation theory close to the critical point in mixtures with strong size asymmetry, e.g. helium–neon.

In summary, the thesis presents accurate semi-classical force fields for ultracryogenic fluids that can be applied in molecular dynamics and Monte Carlo simulations. Considering the high accuracy with which these force fields reproduce the existing experimental measurements, they currently constitute an accurate, predictive and cost-effective modeling approach for obtaining thermodynamic properties of ultracryogenic fluid mixtures.

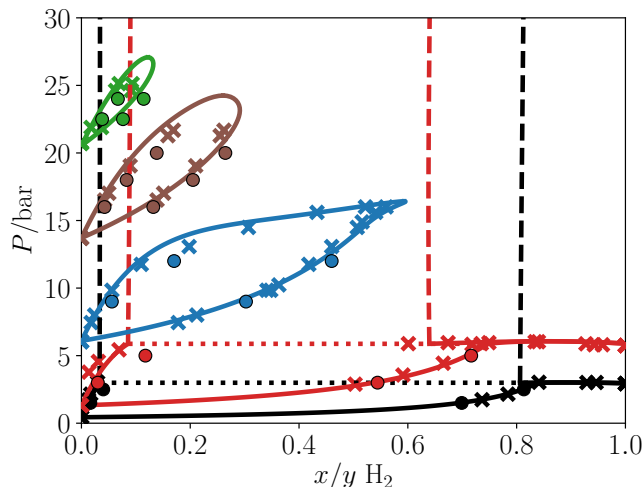


FIG. 3. Phase diagram for the hydrogen-neon mixture. Crosses are experimental measurements^{19,20}, circles are simulation results, and lines are calculations with SAFT-VRQ Mie. The full lines are VLE, the dashed lines are LLE, and the dotted lines indicate VLLE. The temperatures are 24.59 K (black), 28.00 K (red), 34.66 K (blue), 39.57 K (brown) and 42.50 K (green).

C. Applications, extensions and implementation

Being a molecularly based SAFT-type model, two possible extensions of the theory seem natural. One is to cast it in the form of a density functional theory, which should be achievable by following a methodology that is now well-established in the SAFT community. Another extension would be to develop a bulk equation of state for solid phases, based on the semiclassical force field developed here. Solid neon would be of special interest, as it is the quantum fluid with the highest triple point temperature and runs the risk of freezing out, e.g., in heat exchangers of hydrogen liquefaction process designs that use helium–neon mixtures as working fluids.

Quantum swelling – the increase in the apparent size of a molecule as the temperature decreases – has a large impact on the thermodynamic properties of the system as it fundamentally changes the fluid structure. The optimized semiclassical force fields quantify this important effect, which means that they can be used to incorporate quantum swelling into any classical model where the size of the component enters as a parameter. Crucially, this can be done in a completely predictive way without introducing any new fitting parameters. A follow-up work²¹ of the thesis exploited this idea to deduce quantum-corrections to the covolume parameter of cubic equations of state. These turned out to have an enormous impact on accuracy, e.g. by reducing the average error for the saturated isochoric heat capacity of liquid hydrogen from 80% to 4%, and resulted in the first cubic equation of state suitable for ultracryogenic fluids. The direct transferability of the

intermolecular potentials to the cubic EoS confirms the accuracy and usefulness of the potentials.

In the wake of the thesis, the implementation of SAFT-VRQ Mie equation of state was made open source and freely available²²

II. KEY INNOVATION: CURVED INTERFACIAL THERMODYNAMICS FOR MIXTURES

A. Background and state of the art

The foundations of interfacial thermodynamics were put forward by Gibbs²³. He introduced the concept of a dividing surface, which is a hypothetical sharp surface located in the interface region separating the bulk phases. Any extensive property, such as the internal energy, can be written (exactly) as the sum of the bulk values on each side of the dividing surface, plus a *surface excess* that encodes the influence of the surface. Interfacial thermodynamics is the study of these excess properties, and is complicated by the fact that these excesses depend on the position of the dividing surface. The central quantity in interfacial thermodynamics is the surface tension, defined as the excess grand free energy per area of the dividing surface^{24,25}.

The surface tension depends on curvature, and the study of this dependence is an active field^{26–37}. For droplets and bubbles the curvature can be quantified by the inverse radius, $1/R$. To apply the curvature expansion for surface tension a second-order expansion is usually necessary,

$$\sigma^s(R) = \sigma_0 - \frac{2\sigma_0\delta}{R} + \frac{k_s}{R^2} + \mathcal{O}\left(\frac{1}{R^3}\right), \quad (2)$$

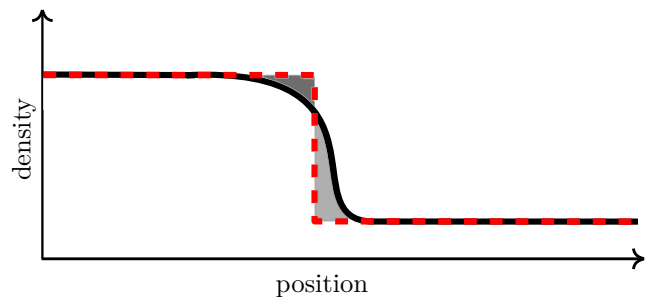


FIG. 4. Illustration of the concept of a dividing surface for the density profile of a planar vapor–liquid interface. The black curve is the true density profile, while the dashed red curve is the density profile assuming a sharp dividing surface. The dividing surface as shown yields a positive excess number of particles, since the light-gray area on the vapor side is larger than the dark-gray area on the liquid side.

which is known as the Helfrich expansion. The first-order correction is given by the Tolman length δ , and the second-order correction is given by the spherical rigidity k_s . Its use has historically focused on pure systems, partly because the theory has not been developed for mixtures.

The main theoretical approach to study interfaces is classical density functional theory (DFT)^{24,38}. In DFT, the free energy of the system is given by a functional of the density profiles of each component, and the equilibrium density profiles are given by minimizing this functional. The simplest realistic DFT is the square gradient theory (SGT), also known as density gradient theory. Originally developed by van der Waals³⁹, SGT was later rederived in many other guises and contexts, and is still widely used today^{24,40,41}. In SGT, the free-energy density equals a bulk term, given by an equation of state, plus a term proportional to the squared gradient of the density profile. The proportionality constant is an empirical parameter usually fitted to measured values of the planar surface tension. More sophisticated DFTs are fully predictive^{36,42–44}, but the predicted planar surface tensions can be highly inaccurate for important substances such as water and alcohols^{35,44}. This is one reason why SGT remains an important research tool.

B. Method and results

A whole chapter of the thesis was dedicated to explaining and presenting the general theory for the curvature dependence of surface tension for mixtures, and calculating the curvature corrections using square gradient theory. The main idea underlying the extension to mixtures is illustrated in Fig. 5. A given physical process yields a path into the metastable state space of a fluid, and this path can be parametrized by the radius R of the equilibrium bubble/droplet at a given state along the path. All thermodynamic properties can then be Taylor-expanded in the curvature $1/R$, which is zero at the binodal. Most central is the Taylor expansion of the surface tension, as given by Eq. (2), as it is directly linked to the free energy of the system. The thesis presented and explained the general theory for the curvature dependence of the surface tension for multicomponent fluids by use of the Helfrich expansion. To exemplify the theory, SGT was employed for a mixture of hexane-heptane at 298.15 K to obtain the quantitative estimates of curvature expansion coefficients along different paths.

The thermodynamic properties along a path are highly dependent on the path. This path-dependence issue is not present for isothermal single-components systems, and the thesis therefore presents the first investigation of the path-dependence of excess properties in the thermodynamic state space of mixtures. It was shown that the choice of path has a decisive impact on the accuracy of the curvature expansion, and that the path of constant bulk

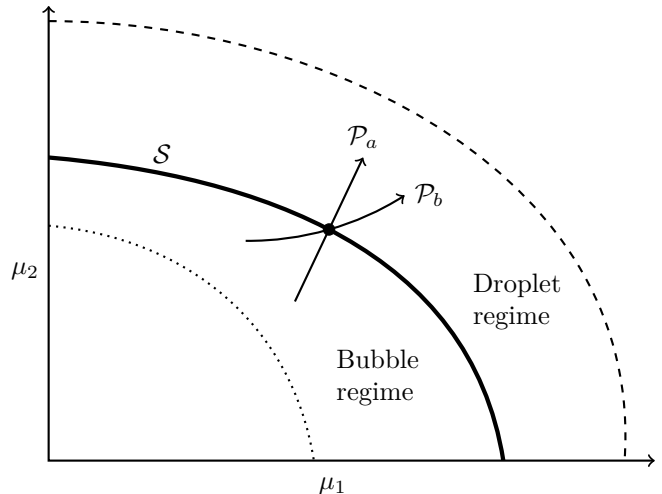


FIG. 5. Two possible paths in chemical potential-space at a fixed temperature, passing through a saturation state (black point), where the liquid surface curvature increases in the indicated direction. The shape of the phase envelope S is typical for vapor–liquid equilibrium of two subcritical components. The dashed and dotted curves indicate the vapor and liquid spinodals, respectively.

liquid composition yields the highest accuracy. For the hexane–heptane mixture, an expansion along this path reproduced the surface tension from SGT within 0.1% for droplet radii down to 3 nanometers.

We also gave detailed attention to the influence of the choice of dividing surface. It is evident from Fig. 4 that this surface is rather arbitrary, and it is useful to know exactly how this choice affects the curvature expansion coefficients. We therefore established transformation formulae for the curvature expansion coefficients for different surfaces. Since these were proven from first principles, they hold true for all thermodynamically consistent treatments of bubbles and droplets. We showed that whereas the Tolman length is independent of the choice of dividing surface, the rigidity constants do and obey a simple transformation law.

C. Application to nucleation in surface-active mixtures

The developed framework is applicable to a wide range of fluid mixtures and can be used to accurately represent the surface tension of nanoscopic bubbles and droplets. A particularly important application of the curvature dependence of surface tension is nucleation theory, a central topic of the thesis. Most first order phase transitions, such as condensation, cavitation, boiling, and crystallization take place through nucleation. Here, the rate-limiting step is the formation of an incipient portion of the new phase

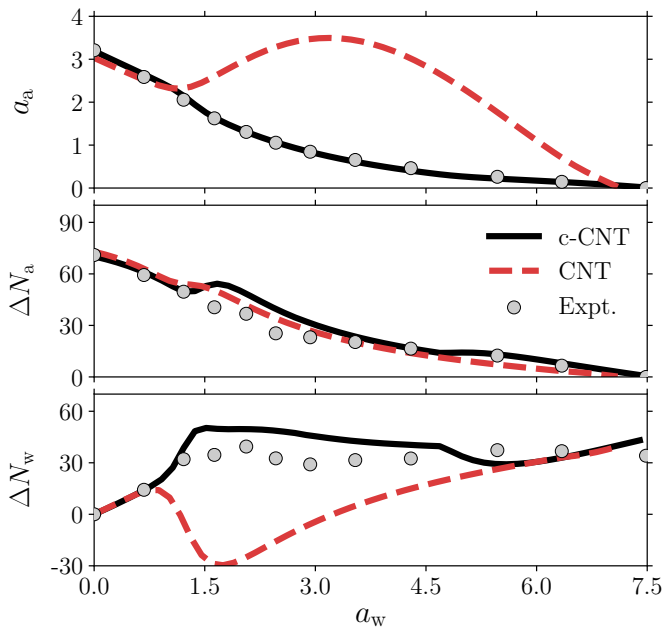


FIG. 6. Properties of critical droplets in the water–ethanol mixture at 260 K calculated for CNT and c-CNT, plotted as a function of water activity in the gas. Experimental data are from Ref. 45. Top: ethanol activities in the gas phase corresponding to onset of condensation. Middle: number of ethanol molecules in the droplets. Bottom: number of water molecules.

exceeding the critical size required to continue growing spontaneously. This qualitative picture of the process is the basis of classical nucleation theory (CNT), which is the most popular model for predicting the rates of formation and properties of nucleating embryos^{47–49}. For *pure* fluids, CNT is qualitatively correct^{50–52}. However, the predicted rates show systematic deviations from experiments, with errors reaching 20 orders of magnitude for argon⁵³. The surface tension crucially affects the work of formation for a critical droplet/bubble^{48,54–59}, and for pure water droplets nucleating in supersaturated vapor, incorporating the curvature dependence of the surface tension improves the agreement between the theory and

TABLE I. Statistics for the logarithmic deviations $\log_{10}(J/J^{\text{expt}})$ from the experimental nucleation rates J^{expt} of Refs. 45 and 46. The average and median are calculated using absolute values of the logarithmic deviations.

Method	min	max	average	median
ethanol–water				
CNT	–21.3	–0.2	10.9	12.7
c-CNT	–2.3	0.9	0.8	0.5
1-propanol–water				
CNT	–35.2	1.5	14.8	9.5
c-CNT	–2.7	2.9	1.5	1.2

the experimental results^{60,61}.

For mixtures incorporation of curvature effects had not been attempted, as the study of nucleation in fluid mixtures exposes challenges beyond those of pure systems. A striking example is homogeneous condensation in highly surface-active water–alcohol mixtures, where classical nucleation theory yields an unphysical, negative number of water molecules in the critical droplet. This flaw has rendered multicomponent classical nucleation theory useless for many industrial and scientific applications.

As a challenging test of the developed framework for treating curvature expansions for mixtures, the thesis therefore attempted to treat the surface-active alkanol–water mixtures in detail. This constituted the first systematic and rigorous approach to modeling the nucleation of surface-active systems. The corrected theory, c-CNT, yielded a striking improvement in the accuracy compared to CNT. As shown in Tab. I, for the ethanol–water and propanol–water mixtures, the average error in the predicted nucleation rates is reduced from 11–15 orders of magnitude to below 1.5. The improvement in the maximum error is much larger, being reduced from 21–35 orders of magnitude to below 3.

More important than the gain in accuracy, it was found that the inconsistency was completely removed by properly incorporating the curvature dependence of the surface tension of the mixture into classical nucleation theory for multicomponent systems. This is illustrated in Fig. 6, where the molecular content of the critical droplets were deduced from rate measurements using the nucleation theorem⁶².

Due to the thermodynamic consistency of the modeling approach, the reason for the negative water content predicted by CNT could be studied in detail. The Gibbs adsorption equation was used to explain the origin of the inconsistency by linking the molecules adsorbed at the interface to the curvature corrections of the surface tension. In particular we derived a correction to the predicted adsorption that is missing in classical nucleation theory:

$$\Delta\Gamma \approx \delta + (4\delta^2 - k_s/\sigma_0)/R. \quad (3)$$

This expression is a salient demonstration of why the curvature dependence of the surface tension is crucial to capturing the adsorptions, to the extent that neglecting it may imply a negative molecular content of one of the components. This is especially important for surface-active mixtures, where Tolman lengths and spherical rigidities can far exceed their pure-component values.

The curvature-corrected nucleation theory opens the door to reliable predictions of nucleation rates in multicomponent systems, which are crucial for applications ranging from atmospheric science to research on volcanos. Possible future directions of research are to apply the curvature correction theory to systems with a liquid–liquid phase split, to mixtures of aerosols and water, or to heteroge-

neous nucleation theory. Especially interesting would be to attempt extending the framework and expressions such as Eq. (3) to crystallization, where the role of the crystal morphology might play a role.

REFERENCES

- ¹E. Wigner, *Phys. Rev.* **40**, 749 (1932)
- ²J. G. Kirkwood, *Phys. Rev.* **44**, 31 (1933)
- ³R. P. Feynman, A. R. Hibbs, and D. F. Styer, *Quantum Mechanics and Path Integrals, Emended edition* (McGraw-Hill, New York, 2005) ISBN 9780486477220, p. 384
- ⁴A. V. A. Kumar, H. Jobic, and S. K. Bhatia, *J. Phys. Chem. B* **110**, 16666 (2006)
- ⁵J. M. Salazar, S. Lectez, C. Gauvin, M. Macaud, J. P. Bellat, G. Weber, I. Bezverkhy, and J. M. Simon, *Int. J. Hydrogen Energy* **42**, 13099 (2017)
- ⁶F. Calvo, J. P. K. Doye, and D. J. Wales, *J. Chem. Phys.* **114**, 7312 (2001)
- ⁷R. Rodríguez-Cantano, R. Pérez de Tudela, M. Bartolomei, M. I. Hernández, J. Campos-Martínez, T. González-Lezana, P. Villarreal, J. Hernández-Rojas, and J. Bretón, *J. Phys. Chem. A* **120**, 5370 (2016)
- ⁸P. Kowalczyk, L. Brualla, P. Gauden, and A. P. Terzyk, *Phys. Chem. Chem. Phys.* **11**, 9182 (2009)
- ⁹V. M. Trejos, A. Gil-Villegas, and A. Martinez, *J. Chem. Phys.* **139**, 184505 (2013)
- ¹⁰R. Span, *Multiparameter Equations of State* (Springer-Verlag, Berlin, 2000)
- ¹¹Ø. Wilhelmsen, A. Aasen, G. Skaugen, P. Aursand, A. Austegard, E. Aursand, M. A. Gjennestad, H. Lund, G. Linga, and M. Hammer, *Ind. Eng. Chem. Res.* **56**, 3503 (2017)
- ¹²Ø. Wilhelmsen, D. Berstad, A. Aasen, P. Nekså, and G. Skaugen, *Int. J. Hydrogen Energy* **43**, 5033 (2018)
- ¹³G. Soave, *Chem. Eng. Sci.* **27**, 1197 (1972)
- ¹⁴D. Y. Peng and D. B. Robinson, *Ind. Eng. Chem. Fund.* **15**, 59 (1976)
- ¹⁵M.-J. Huron and J. Vidal, *Fluid Phase Equilib.* **3**, 255 (1979)
- ¹⁶O. Jørstad, *Equations of State for Hydrocarbon Mixtures*, PhD dissertation, Norwegian Institute of Technology (NTH) (1993)
- ¹⁷J. Gross and G. Sadowski, *Ind. Eng. Chem. Res.* **40**, 1244 (2001)
- ¹⁸J. A. Barker and D. Henderson, *Rev. Mod. Phys.* **48**, 587 (1976)
- ¹⁹W. B. Streett and C. H. Jones, *J. Chem. Phys.* **42**, 3989 (1965)
- ²⁰C. K. Heck and P. Barrick, in *Adv. Cryog. Eng.* (Springer, 1966) pp. 349–355
- ²¹A. Aasen, M. Hammer, S. Lasala, J.-N. Jaubert, and Ø. Wilhelmsen, *Fluid Phase Equilib.* **524**, 112790 (2020)
- ²²SINTEF Energy Research, “Thermopack open source thermodynamics library,” <https://github.com/SINTEF/thermopack/> (2020)
- ²³J. Gibbs, *The Scientific Papers of J. Willard Gibbs* (Ox Bow Press, London, 1993)
- ²⁴J. Rowlinson and B. Widom, *Molecular Theory of Capillarity* (Clarendon Press, Oxford, 1984)
- ²⁵A. Malijevský and G. Jackson, *J. Phys.: Condens. Matter* **24**, 464121 (2012)
- ²⁶R. C. Tolman, *J. Chem. Phys.* **17**, 333 (1949)
- ²⁷A. E. van Giessen and E. M. Blokhuis, *J. Chem. Phys.* **116**, 302 (2002)
- ²⁸Y. A. Lei, T. Bykov, S. Yoo, and X. C. Zeng, *J. Am. Chem. Soc.* **127**, 15346 (2005)
- ²⁹Z. Li and J. Wu, *Ind. Eng. Chem. Res.* **47**, 4988 (2008)
- ³⁰A. E. van Giessen and E. M. Blokhuis, *J. Chem. Phys.* **131**, 164705 (2009)
- ³¹J. G. Sampayo, A. Malijevský, E. A. Müller, E. de Miguel, and G. Jackson, *J. Chem. Phys.* **132**, 141101 (2010)
- ³²B. J. Block, S. K. Das, M. Oettel, P. Virnau, and K. Binder, *J. Chem. Phys.* **133**, 154702 (2010)
- ³³A. Tröster, M. Oettel, B. Block, P. Virnau, and K. Binder, *J. Chem. Phys.* **136**, 064709 (2012)
- ³⁴M. Horsch, H. Hasse, A. K. Shchekin, A. Agarwal, S. Eckelsbach, J. Vrabc, E. A. Müller, and G. Jackson, *Phys. Rev. E* **85**, 031605 (2012)
- ³⁵P. Rehner, A. Aasen, and Ø. Wilhelmsen, *J. Chem. Phys.* **151**, 244710 (2019)
- ³⁶P. Rehner and J. Gross, *J. Chem. Phys.* **148**, 164703 (2018)
- ³⁷S. Kim, D. Kim, J. Kim, S. An, and W. Jhe, *Phys. Rev. X* **8**, 041046 (2018)
- ³⁸J.-P. Hansen and I. R. McDonald, *Theory of simple liquids: with applications to soft matter* (Academic Press, 2013)
- ³⁹J. D. van der Waals, *J. Stat. Phys.* **20**, 200 (1979)
- ⁴⁰A. Aasen, E. M. Blokhuis, and Ø. Wilhelmsen, *J. Chem. Phys.* **148**, 204702 (2018)
- ⁴¹E. M. Blokhuis and A. E. van Giessen, *J. Phys.: Condens. Matter* **25**, 225003 (2013)
- ⁴²J. Gross, *J. Chem. Phys.* **131**, 204705 (2009)
- ⁴³P. Rehner and J. Gross, *Phys. Rev. E* **98**, 063312 (2018)
- ⁴⁴J. Algaba, J. M. Míguez, B. Mendiboure, and F. J. Blas, *Phys. Chem. Chem. Phys.* **21**, 11937 (2019)
- ⁴⁵Y. Viisanen, R. Strey, A. Laaksonen, and M. Kulmala, *J. Chem. Phys.* **100**, 6062 (1994)
- ⁴⁶R. Strey, Y. Viisanen, and P. Wagner, *J. Chem. Phys.* **103**, 4333 (1995)
- ⁴⁷D. Kashchiev, *Nucleation: Basic Theory with Applications* (Butterworth–Heinemann, Oxford, 2000)
- ⁴⁸H. Vehkamäki, *Classical Nucleation Theory in Multicomponent Systems* (Springer Verlag, Berlin, 2006)
- ⁴⁹V. Kalikmanov, *Nucleation Theory* (Springer Verlag, Berlin, 2013)
- ⁵⁰Y. Viisanen, R. Strey, and H. Reiss, *J. Chem. Phys.* **99**, 4680 (1993)
- ⁵¹J. Wedekind, D. Reguera, and R. Strey, *J. Chem. Phys.* **127**, 064501 (2007)
- ⁵²R. McGraw and A. Laaksonen, *Phys. Rev. Lett.* **76**, 2754 (1996)
- ⁵³K. Iland, J. Wölk, R. Strey, and D. Kashchiev, *J. Chem. Phys.* **127**, 154506 (2007)
- ⁵⁴J. Schmelzer, I. Gutzow, and J. J. Schmelzer, *J. Colloid Interf. Sci.* **178**, 657 (1996)
- ⁵⁵P. Debenedetti, *Metastable Liquids: Concepts and Principles* (Princeton University Press, Princeton, 1996)
- ⁵⁶N. Bruot and F. Caupin, *Phys. Rev. Lett.* **116**, 056102 (2016)
- ⁵⁷V. G. Baidakov, S. P. Protsenko, and V. M. Bryukhanov, *Chem. Phys. Lett.* **663**, 57 (2016)
- ⁵⁸T. Hiratsuka, H. Tanaka, and M. T. Miyahara, *J. Phys. Chem. C* **121**, 26877 (2017)
- ⁵⁹B. Cheng, G. A. Tribello, and M. Ceriotti, *J. Chem. Phys.* **147**, 104707 (2017)
- ⁶⁰Ø. Wilhelmsen, D. Bedeaux, and D. Reguera, *J. Chem. Phys.* **142**, 171103 (2015)
- ⁶¹M. N. Joswiak, R. Do, M. F. Doherty, and B. Peters, *J. Chem. Phys.* **145**, 204703 (2016)
- ⁶²D. Kashchiev, *J. Chem. Phys.* **76**, 5098 (1982)